

Seeing the magnetic monopole through the mirror of topological surface states

Xiao-Liang Qi¹, Rundong Li¹, Jiadong Zang² and Shou-Cheng Zhang^{1,2}¹*Department of Physics, Stanford University, Stanford, CA 94305-4045*²*Department of Physics, Fudan University, Shanghai, 200433, China*

(Dated: November 8, 2008)

Existence of the magnetic monopole is compatible with the fundamental laws of nature, however, this illusive particle has yet to be detected experimentally. In this work, we show that an electric charge near the topological surface state induces an image magnetic monopole charge due to the topological magneto-electric effect. The magnetic field generated by the image magnetic monopole can be experimentally measured, and the inverse square law of the field dependence can be determined quantitatively. We propose that this effect can be used to experimentally realize a gas of quantum particles carrying fractional statistics, consisting of the bound states of the electric charge and the image magnetic monopole charge.

The electromagnetic response of a conventional insulator is described by a dielectric constant ϵ and a magnetic permeability μ . An electric field induces an electric polarization, while a magnetic field induces a magnetic polarization. Since both the electric field $\mathbf{E}(x)$ and the magnetic field $\mathbf{B}(x)$ are well defined inside an insulator, the linear response of a conventional insulator can be fully described by the effective action $S_0 = \int d^3x dt (\epsilon \mathbf{E}^2 - \frac{1}{\mu} \mathbf{B}^2)$. However, in general, another possible term is allowed in the effective action, which is quadratic in the electromagnetic field, contains the same number of derivatives of the electromagnetic potential, and is rotationally invariant; it is given by $S_\theta = \frac{\theta}{2\pi} \frac{\alpha}{2\pi} \int d^3x dt \mathbf{E} \cdot \mathbf{B}$. Here $\alpha = e^2/\hbar c$ is the fine structure constant, and θ can be viewed as a phenomenological parameter in the sense of the effective Landau-Ginzburg theory. This term describes the magneto-electric effect¹, where an electric field can induce a magnetic polarization, and a magnetic field can induce an electric polarization.

Unlike conventional terms in the Landau-Ginzburg effective actions, the integrand in S_θ is a total derivative term, when $\mathbf{E}(x)$ and $\mathbf{B}(x)$ are expressed in terms of the electromagnetic vector potential:

$$\begin{aligned} S_\theta &= \frac{\theta}{2\pi} \frac{\alpha}{16\pi} \int d^3x dt \epsilon_{\mu\nu\rho\tau} F^{\mu\nu} F^{\rho\tau} \\ &= \frac{\theta}{2\pi} \frac{\alpha}{4\pi} \int d^3x dt \partial^\mu (\epsilon_{\mu\nu\rho\sigma} A^\nu \partial^\rho A^\sigma) \end{aligned} \quad (1)$$

Furthermore, when periodic boundary condition is imposed in both the spatial and temporal directions, the integral of such a total derivative term is always quantized to be an integer, *i.e.* $S_\theta/\hbar = \theta n$. Therefore, the partition function and all physically measurable quantities are invariant when the θ parameter is shifted by 2π times an integer. Under time reversal symmetry, $e^{i\theta n}$ is transformed into $e^{-i\theta n}$. Therefore, all time reversal invariant insulators fall into two general classes, either described by $\theta = 0$ or by $\theta = \pi^2$. These two time reversal invariant classes are disconnected, and they can only be connected continuously by time-reversal breaking perturbations. This classification of time reversal invariant insulators in terms of the two possible values of the θ

parameter is generally valid for insulators with arbitrary interactions². The effective action contains the complete description of the electromagnetic response of topological insulators. In Ref.², it was shown that such a general definition of a topological insulator reduces to the Z_2 topological insulators described in Ref.^{3,4,5} for non-interacting band insulators, which is a 3D generalization of the quantum spin Hall insulator in 2D^{6,7,8,9}. Recently, experimental evidence of the topologically non-trivial surface states³ has been observed in $Bi_{1-x}Sb_x$ alloy¹⁰.

With periodic temporal and spatial boundary conditions, the partition function is periodic in θ under the 2π shift, and the system is invariant under the time reversal symmetry at $\theta = 0$ and $\theta = \pi$. However, with open boundary conditions, the partition function is no longer periodic in θ , and time reversal symmetry is generally broken, but only on the boundary, even when $\theta = (2n + 1)\pi$. Ref.² gives the following physical interpretation. Time reversal invariant topological insulators have a bulk energy gap, but have gapless excitations with an odd number of Dirac cones on the surface. When the surface is coated with a thin magnetic film, time reversal symmetry is broken, and an energy gap also opens up at the surface. In this case, the low energy theory is completely determined by the surface term in Eq. (1). Since the surface term is a Chern-Simons term, it describes the quantum Hall effect on the surface. From the general Chern-Simons-Landau-Ginzburg theory of the quantum Hall effect¹¹, we know that the coefficient $\theta = (2n + 1)\pi$ gives a quantized Hall conductance of $\sigma_{xy} = (n + \frac{1}{2})e^2/\hbar$. This quantized Hall effect on the surface is the physical origin behind the topological magneto-electric (TME) effect. Under an applied electric field, a quantized Hall current is induced on the surface, which in turn generates a magnetic polarization, and vice versa.

In this work, we point out a profound manifestation of the TME effect. When a charged particle is brought close to the surface of a topological insulator, a magnetic monopole charge is induced as a mirror image of the electric charge. The full set of electromagnetic field equations can be obtained from the functional variation of the action $S_0 + S_\theta$, and they are similar to the equations of

axion electro-dynamics in particle physics¹². They can be presented as conventional Maxwell's equations, but with the modified constituent equations describing the TME effect²:

$$\mathbf{D} = \mathbf{E} + 4\pi\mathbf{P} - 2\alpha P_3\mathbf{B} \quad , \quad \mathbf{H} = \mathbf{B} - 4\pi\mathbf{M} + 2\alpha P_3\mathbf{E} \quad (2)$$

where $P_3(x) = \theta(x)/2\pi$ is the electro-magnetic polarization introduced in Ref.². It takes the value of $P_3 = 0$ in vacuum or conventional insulators, and $P_3 = \pm 1/2$ in topological insulators, with the sign determined by the direction of the surface magnetization.

Now consider the geometry as shown in Fig.1. The lower half space ($z < 0$) is occupied by a topological insulator with a dielectric constant ϵ_2 and a magnetic permeability μ_2 , while the upper half space ($z > 0$) is occupied by a conventional insulator with a dielectric constant ϵ_1 and a magnetic permeability μ_1 . A point electric charge q is located at $(0, 0, d)$ with $d > 0$. The Maxwell's equation, along with the modified constituent equations and the standard boundary conditions, constitute a complete boundary value problem. To solve this problem, the method of images¹³ can be employed. Let us assume in the lower half space the electric field is given by an effective point charge q/ϵ_1 and an image charge q_1 at $(0, 0, d)$, whereas the magnetic field is given by an image magnetic monopole g_1 at $(0, 0, d)$. In the upper half space the electric field is given by an electric charge q/ϵ_1 at $(0, 0, d)$ and an image charge q_2 at $(0, 0, -d)$, the magnetic field is given by an image magnetic monopole g_2 at $(0, 0, -d)$. It is easily seen that the above ansatz satisfies the Maxwell's equation on each side of the boundary. At the boundary $z = 0$ the solution is then matched according to the standard boundary condition, giving

$$\begin{aligned} q_1 &= q_2 = \frac{1}{\epsilon_1} \frac{(\epsilon_1 - \epsilon_2)(1/\mu_1 + 1/\mu_2) - 4\alpha^2 P_3^2}{(\epsilon_1 + \epsilon_2)(1/\mu_1 + 1/\mu_2) + 4\alpha^2 P_3^2} q \\ g_1 &= -g_2 = -\frac{4\alpha P_3}{(\epsilon_1 + \epsilon_2)(1/\mu_1 + 1/\mu_2) + 4\alpha^2 P_3^2} q. \end{aligned} \quad (3)$$

To see the physics more clearly, we will first take $\epsilon_1 = \epsilon_2 = \mu_1 = \mu_2 = 1$ below, and then recover the $\epsilon_{1,2}$, $\mu_{1,2}$ when discussing the experimental proposals later. The solution above shows that for an electric charge near the surface of a topological insulator, both an image magnetic monopole and an image electric charge will be induced, as compared with conventional electromagnetic media where only an electric image charge will be induced. It is remarkable that the magnitude of the image magnetic monopole and image electric charge satisfy the relation $q_{1,2} = \pm(\alpha P_3)g_{1,2}$. This is just the relation $q = (\theta/2\pi)g$ derived by Witten¹⁴, for the electric and magnetic charges of a dyon inside the θ vacuum, with $\theta/2\pi = \pm P_3$ here.

The physical origin of the image magnetic monopole is understood by rewriting part of the Maxwell's equation as

$$\nabla \times \mathbf{B} = 2\alpha P_3 \delta(z) \hat{\mathbf{n}} \times \mathbf{E}. \quad (4)$$

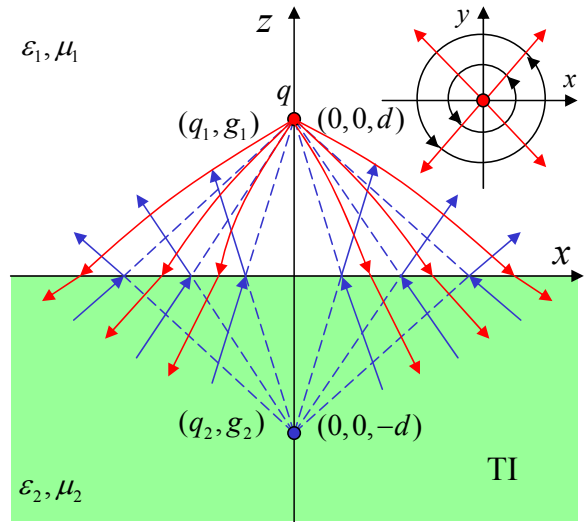


FIG. 1: Illustration of the image electric charge and the image monopole of a point-like electric charge. The lower half space is occupied by a topological insulator (TI) with dielectric constant ϵ_2 and magnetic permeability μ_2 . The upper half space is occupied by a topologically trivial insulator (or vacuum) with dielectric constant ϵ_1 and magnetic permeability μ_1 . A point electric charge q is located at $(0, 0, d)$. Seen from the lower half space, the image electric charge q_1 and magnetic monopole g_1 are at $(0, 0, d)$. Seen from the upper half space, the image electric charge q_2 and magnetic monopole g_2 are at $(0, 0, -d)$. The red (blue) solid lines represent the electric (magnetic) field lines. The inset is a top-down view showing the in-plane component of the electric field at the surface (red arrows) and the circulating surface current (black circles).

with $P_3 = \pm 1/2$ the value for the topological insulator. The right hand side of the above equation corresponds to a surface current density $\mathbf{j} = \sigma_{xy}(\hat{\mathbf{n}} \times \mathbf{E})$, which is induced by the in-plane component of the electric field and is perpendicular to it. This current is nothing but the quantized Hall current mentioned earlier. For the problem under consideration, the surface current density is calculated as

$$\mathbf{j} = P_3 \left(\frac{e^2}{h} \right) \left(\frac{q}{1 + \alpha^2 P_3^2} \right) \frac{r}{(r^2 + d^2)^{\frac{3}{2}}} \hat{\mathbf{e}}_\varphi, \quad (5)$$

which is circulating around the origin as shown in the inset of Fig.1. Physically, this surface current is the source that induces the magnetic field. On each side of the surface, the magnetic field induced by the surface current can be viewed as the field induced by an image magnetic monopole on the opposite side.

From the above calculation we clearly see that the image magnetic monopole field indeed has the correct magnetic field dependence expected from a monopole, and it can be controlled completely through the position of the electric charge. Since we started with the Maxwell's equation, which includes $\nabla \cdot \mathbf{B} = 0$, the magnetic flux

integrated over a closed surface must vanish. We can indeed check that this is the case by considering a closed surface, for example a sphere with radius a , which encloses a topological insulator. Inside the closed surface, there is not only a image magnetic monopole charge, but also a line of magnetic charge density whose integral exactly cancels the point image magnetic monopole. However, when the separation between the electric charge and the surface, d , is much smaller than the spherical radius a , the magnetic field is completely dominated by the image magnetic monopole, and the contribution due to the line of magnetic charge density is vanishingly small. Therefore, we propose here to experimentally observe the magnetic monopole in the same sense as we can experimentally observe other fractionalization, or deconfinement, phenomena in condensed matter physics. In any closed electronic system, the total charge must be quantized to be an integer. However, one can separate fractionally charged elementary excitations arbitrarily far from each other, so that fractional charge can have well defined meaning locally. Similar situation occurs in spin-charge separation. While the total charge and the total spin of a closed system must be linked to each other, spin and charge can occur as well separated local excitations. In our case, as long as d is much smaller than the radius of curvature of a topological surface a , the local magnetic field is completely determined by a single image magnetic monopole.

Such an image monopole can be observed experimentally by a Magnetic Force Microscope (MFM). Consider the surface of the topological insulator with a localized charged impurity, as shown in Fig. 2. A scanning MFM tip can be applied to detect the magnetic field distribution of the image monopole. However, the charge of the impurity also generates an electric force to the tip. Here we show that the contribution of the image monopole can be distinguished from other trivial contributions by scanning both the tip position r and the tip voltage V . For a given position r , we define $f_{\min}(r)$ as the minimal force applied to the tip when scanning the voltage. Denote the distance of the charged impurity to the surface as D , in the limit of $r \gg D$ the conventional charge interaction leads to a $1/r^6$ dependence of $f_{\min}(r)$. On comparison, the image monopole magnetic field leads to more dominant contribution

$$f_{\min}(r) \simeq \frac{4\alpha P_3}{(1 + \epsilon_2/\epsilon_1)(1/\mu_1 + 1/\mu_2) - 4\alpha^2 P_3^2} \frac{Q\phi}{r^3} \quad (6)$$

in which Q is the impurity charge and ϕ is the net flux of the magnetic tip. For the estimated parameters $\epsilon_2 \simeq 100$ for $\text{Bi}_{1-x}\text{Sb}_x$ alloy¹⁵, $\epsilon_1 = 1$, $\mu_1 \simeq \mu_2 \simeq 1$, $\phi \simeq 2.5hc/e$ and a typical distance $r = 50\text{nm}$, the force is $f_{\min}(r) \simeq 0.3pN/\mu m$, which is observable in the present experiments.

When we consider more than one point charges on the surface, the existence of such an image monopole has another important consequence. When an electron is moving on the surface of the topological insulator, it is al-

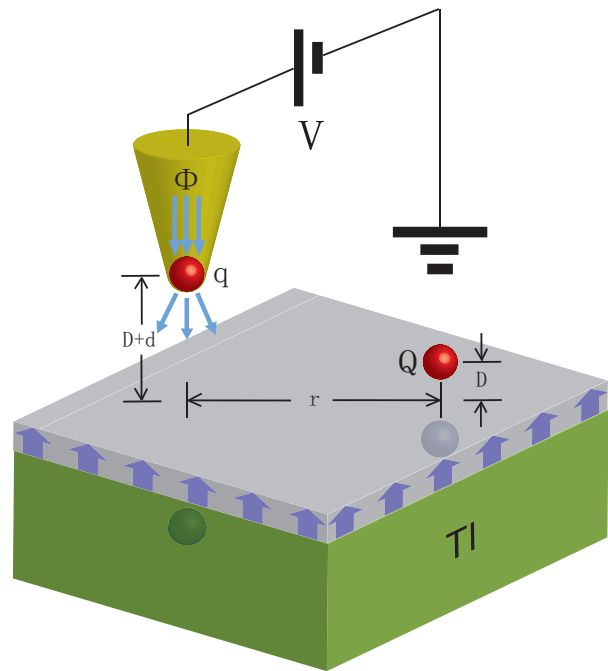


FIG. 2: Illustration of the experimental setting to measure the image monopole. A magnetic layer is deposited on the surface of the topological insulator, as indicated by the layer with blue arrows. (The same layer is drawn in Fig. 3 and 4.) A scanning MFM tip carries a magnetic flux ϕ and a charge q . A charged impurity is confined on the surface with charge Q and distance D to the surface. By scanning over the voltage V and the distance r to the impurity, the effect of the image monopole magnetic field can be measured (see text).

ways followed by its image monopole. In other words, each electron behaves like a bound state of charge and monopole, which is known in the high energy physics as a “dyon”¹⁴. When two dyons are exchanged, each of them will obtain an Aharonov-Bohm (AB) phase due to the magnetic field of the other one. Interestingly, the net AB phase obtained by the two-particle system during an exchange process is independent of the path of the particles on the 2D plane, which thus can be interpreted as a statistical angle of the dyon. Therefore, this setup provides a condensed matter realization of the anyon concept^{16,17} in the absence of any external magnetic field. This effect also provides a mechanism of statistical transmutation in $(3 + 1)$ dimensions^{18,19}. If each dyon has charge q and monopole flux g , then the statistical angle is given by

$$\theta = \frac{gq}{2\hbar c} \quad (7)$$

For example, the binding of an electron with charge e and a monopole with flux hc/e leads to $\theta = \pi$, in which case the dyon is a boson. However, there is an interesting difference between the dyon we studied here and that in high energy physics. In high energy physics the charged particle and monopole are point like particles moving in the 3D. Consequently, the monopole flux must be quantized in unit of hc/e , and correspondingly, the statistical

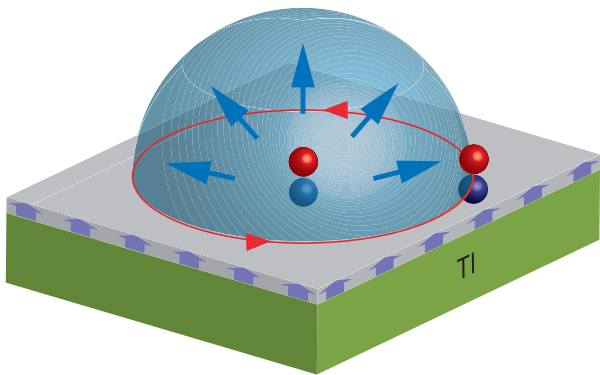


FIG. 3: Illustration of the fractional statistics induced by the image monopole effect. Each electron forms a “dyon” with its image monopole. When two electrons are exchanged, a Aharonov-Bohm phase factor is obtained, which is determined by half of the image monopole flux independent of the exchange path, leading to the phenomenon of statistical transmutation.

angle θ can only be 0 or π modular 2π . This is consistent with the fact that there is no anyonic statistics in $(3+1)$ dimensions. On comparison, our dyon can only be defined if an electron is moving closed to the surface of a topological insulator. Consequently, the “dyon” is always confined on a 2D surface. In this case, the flux of the image monopole does not have to be quantized, and correspondingly, the “dyon” can have anyonic statistics. According to Eq. (3), the statistical angle of an electron-induced dyon is

$$\theta = \frac{2\alpha^2 P_3}{(\epsilon_1 + \epsilon_2)(1/\mu_1 + 1/\mu_2) + 4\alpha^2 P_3^2} \quad (8)$$

For $P_3 = 1/2$ and $\epsilon_1, \mu_1, \mu_2 \sim 1$, $\epsilon_2 \sim 100$, we obtain $\theta \simeq \alpha^2/200 \simeq 2.6 \times 10^{-7}$ rad. Though the statistical angle is quite small, it is physically observable. Consider the geometry as shown in Fig. 4. A quasi 1D superconducting ring and a metallic island surrounded by the ring are deposited on top of the topological insulator surface (which has already been gapped by a magnetic layer). By tuning the gate voltage of the central island, the number of electrons N on the island can be tuned. Due to the statistical angle θ given by Eq. (8), each electron in the central island induces a flux of θ seen by the electrons in the ring. Consequently, the net flux through the ring is $N\theta$ in unit of the flux quanta, which generates a supercurrent in the superconducting ring as in standard Superconducting Quantum Interference Device (SQUID). For a typical electron density of $n = 10^{11}/\text{cm}^2$ and island size $R = 1\mu\text{m}$, the net magnetic flux is $n\theta\pi R^2\hbar c/e \simeq 2.6 \times 10^{-4}\hbar c/2e$ and the correspond-

ing magnetic field is $B = n\theta\hbar c/e \simeq 1.7 \times 10^{-3}\text{G}$, which is observable for SQUID today. It is possible to have some other topological insulator material with a smaller dielectric constant ϵ_2 , in which the statistical angle of dyon can be larger.

In summary, in this paper we have demonstrated that

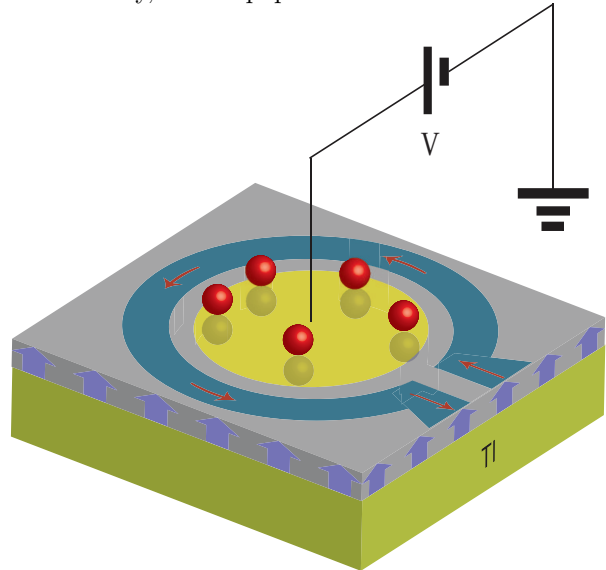


FIG. 4: Illustration of the experimental proposal measuring the fractional statistics of the dyons. When a gate voltage is applied to the central metallic island, the number of electrons in the central island can be tuned, which in turn changes the net flux threaded in the superconducting ring and leads to a supercurrent.

the topological surface states of a 3D topological insulator act as a mirror which images an electron as a monopole. Such a transmutation between electric field and magnetic field is a direct manifestation of the TME effect discussed in Ref.². Due to this effect, a 2D electron gas in the neighborhood of the surface will become a “dyon” gas with fractional statistics. Exotic particles such as the magnetic monopole, dyon, anyon, and the axion have played fundamental roles in our theoretical understanding of quantum physics. Experimental observation of these exotic particles in table top condensed matter systems could finally reveal their deep mysteries.

We wish to thank T. L. Hughes, L. Luan and O. M. Auslaender for insightful discussions. This work is supported by the NSF through the grants DMR-0342832, and by the US Department of Energy, Office of Basic Energy Sciences under contract DE-AC03-76SF00515, and by the Ministry of Education of China under the Grant No. B06011.

¹ L. D. Landau and E. M. Lifshitz, *Electrodynamics of Continuous Media* (Pergamon Press, 1984).

² X. L. Qi, T. Hughes, and S. C. Zhang, arxiv: cond-

- mat/0802.3537.
- ³ L. Fu and C. L. Kane, Phys. Rev. B **74**, 195312 (2006).
 - ⁴ J. E. Moore and L. Balents, Phys. Rev. B **75**, 121306 (2007).
 - ⁵ R. Roy, arxiv: cond-mat/0604211.
 - ⁶ C. L. Kane and E. J. Mele, Phys. Rev. Lett. **95**, 226801 (2005).
 - ⁷ B.A. Bernevig and S.C. Zhang, Phys. Rev. Lett. **96**, 106802 (2006).
 - ⁸ B. A. Bernevig, T. L. Hughes, and S.C. Zhang, Science **314**, 1757 (2006).
 - ⁹ M. König, S. Wiedmann, C. Brüne, A. Roth, H. Buhmann, L. Molenkamp, X.-L. Qi, and S.-C. Zhang, Science **318**, 766 (2007).
 - ¹⁰ D. Hsieh, D. Qian, L. Wray, Y. Xia, Y. S. Hor, R. J. Cava, and M. Z. Hasan, Nature **452**, 970 (2008), ISSN 0028-0836, URL <http://dx.doi.org/10.1038/nature06843>.
 - ¹¹ S. C. Zhang, T. H. Hansson, and S. Kivelson, Phys. Rev. Lett. **62**, 82 (1989).
 - ¹² F. Wilczek, Phys. Rev. Lett. **58**, 1799 (1987).
 - ¹³ J. D. Jackson, *Classical Electrodynamics* (John Wiley, New York, 1999).
 - ¹⁴ E. Witten, Phys. Lett. B **86**, 283 (1979).
 - ¹⁵ O. Madelung, U. Rössler, and M. Schulz, Bi_{1-x}Sb_x optical properties, dielectric constant, in Landolt-Börnstein, Substance/Property Index, Semiconductors, Non-tetrahedrally Bonded Elements and Binary Compounds I, Subvolume III/17E-17F-41C, Springer, Berlin, 1998, pp.1-11.
 - ¹⁶ J. Leinaas and J. Myrheim, Nuovo Cimento B **37**, 1 (1977).
 - ¹⁷ F. Wilczek, Phys. Rev. Lett. **49**, 957 (1982).
 - ¹⁸ R. Jackiw and C. Rebbi, Phys. Rev. Lett. **36**, 1116 (1976).
 - ¹⁹ P. Hasenfratz and G. 't Hooft, Phys. Rev. Lett. **36**, 1119 (1976).